Lanczos Subspace Time-Independent Wave Packet Calculations of S (^{1}D) + H_2 Reactive Scattering

Hong Zhang and Sean C. Smith*

Department of Chemistry, School of Molecular and Microbial Sciences, The University of Queensland, Qld 4072, Brisbane, Australia

Received: October 22, 2001; In Final Form: March 19, 2002

In this paper, we present the results of quantum dynamical simulations of the S (^{1}D) + H_2 insertion reaction on a newly developed potential energy surface (*J. Chem. Phys.* **2001**, *114*, 320). State-to-state reaction probabilities, product state distributions, and initial-state resolved cumulative reaction probabilities from a given incoming reactant channel are obtained from a time-independent wave packet analysis, performed within a single Lanczos subspace. Integral reaction cross sections are then estimated by *J*-shifting method and compared with the results from molecular beam experiment and QCT calculations.

1. Introduction

The dynamics of an insertion reaction are more complicated than a direct abstraction or exchange reaction because insertion reactions usually involve the formation of relatively long-lived complexes characterized by the existence of a deep potential well. Such complexes, considered in isolation, support an intricate resonance structure in the unbound part of their spectrum. This resonance structure dominates the scattering state space of the insertion reaction and makes the quantum simulation of the dynamics very challenging. The H_2 + O (^{1}D) reaction has often been regarded as a benchmark system for studying insertion reactions. Molecular beam and bulk experiments[1−12] have yielded detailed scattering information for a variety of initial states, isotopes, and final state observables. Dynamics calculations employing quasi-classical trajectory (QCT),[13−17] trajectory surface hopping,[18−21] and quantum scattering theory[22−27] have been applied to analyze the detailed reaction dynamics on several high quality ab initio potential energy surfaces (PES).[28−31] Although the insertion mechanism clearly plays a major role in the dynamics, an additional abstraction pathway above about 2 kcal/mol has complicated this reaction. Multiple potential surface effects might be important in accurate simulation of such a reaction, especially for higher collision energies. This has also restricted one from further detailed studies of insertion dynamics in general, e. g., how the dynamics changes as the initial collision energy increases.

Recently, both experiment[32,33] and theory[34−36] indicate that an analogue reaction H_2 + S (^{1}D) may provide a desirable prototype for the insertion mechanism over a wider energy range. Experimentally, Lee and Liu[32,33] have carried out molecular beam experiments over the collision energy range from 0.6 to about 4.1 kcal/mol. The excitation function measurements strongly suggest that the reaction cross section can be entirely attributed to the insertion mechanism in this energy range. Theoretically, a new potential energy surface for H_2 + S (^{1}D) is developed,[35] which is based upon extensive ab initio calculations. The calculations have been performed at a sufficient range of geometries in the entrance and exit channels to enable simulation of the scattering dynamics. A global representation of the lowest PES for H_2 + S (^{1}D) was presented employing both the reproducing kernel Hilbert space (RKHS) method[30,37] and the Murrell−Carter fitting scheme.[29] On the new potential energy surface, Chao and Skodje[34] have performed quasi-classical trajectory (QCT) calculations. Some aspects of the results were clearly consistent with the simple statistical capture/decay model for insertion reaction. However, the more highly resolved quantities (i.e., differential cross sections) displayed features indicative of some nonstatistical reaction dynamics. Comparison of QCT calculations to the molecular beam experiments showed agreements in the broad pattern of the results, but at the same time exhibits significant differences in the more finely resolved quantities. At this point, further quantum mechanical calculations are needed to investigate the reaction mechanism in more detail.

For large molecular systems with a deep potential well, iterative matrix methods such as Chebyshev or Lanczos propagations are suitable choices because they do not require explicit storage of the Hamiltonian matrix, rather only the multiplication of the Hamiltonian onto a vector. When combined with a sparse representation of the Hamiltonian such as a discrete variable representation (DVR),[38] both memory and CPU time can be reduced dramatically. The concept of wave packet scattering was first extended to time-independent iterative methods by Kouri and co-workers.[39−41] They derived a time-independent (TI) wave packet-Lippmann-Schwinger equation and presented a Chebyshev expansion expression of the causal Green operator**.** Mandelshtam and Taylor[42−44] later introduced a very efficient scheme to implement dissipative boundary conditions with a real damped Chebychev recursion, which has enabled very significant computational advances. Guo and Chen,[45,46] Neuhauser et al.,[47−49] and Gray and Balint-Kurti[50,51] have developed related efficient real Chebyshev approaches. Very recently, Zhang and Smith[52] recast the time-independent wave packet-Lippmann-Schwinger equation of Kouri et al. into a Lanczos representation and implemented an efficient Lanczos subspace time-independent wave packet method. In this Lanczos subspace method, we transform the primary Hamiltonian into a tridiagonal representation. Under this representation, we implement the action of the Green operator by solving a

* To whom correspondence should be addressed. Fax: 61-7-3365-7562. E-mail: s.smith@chemistry.uq.edu.au.

10.1021/jp0139181 CCC: $22.00
Published on Web 06/01/2002

tridiagonal linear system with a *QR* algorithm to extract all state to state scattering information. This method is an extension of Lanczos subspace filter diagonalization methods[53−57] which we have developed in recent years.

In this paper, we will apply the Lanczos subspace time-independent wave packet method to the bimolecular reactive scattering of $H_2 + S$ (^1D). The article is organized as follows: we present the outline of the Lanczos TI wave packet method in section 2, and then in section 3, we present the results of the three-dimensional quantum mechanical calculations of S (^1D) + H_2 reactive scattering for $J = 0$. By using *J*-shifting method[58,59] the integral reaction cross sections are estimated and compared with the crossed beam experimental data and quasiclassical trajectory results. Section 4 concludes.

2. Methodology

As discussed by Tannor, Kouri, Zhang, and others, **S** matrix elements can be expressed in terms of the causal Green's function (see[60−64])

$$S_{\beta\alpha}(E) = \frac{i}{2\pi a_\alpha(E) a_\beta^*(E)} \langle \chi_\beta | \hat{G}^+(E) | \chi_\alpha \rangle \tag{1}$$

Three specific equations for **S** matrix elements exist, among which we use the scattering amplitude expression since it is the simplest one to use when combined with the product Jacobi coordinates

$$S_{\beta\alpha}(E) = \frac{1}{a_\alpha(E)} \sqrt{\frac{2\pi\hbar k_\beta}{\mu_\beta}} e^{-ik_\beta R_\infty} \langle \varphi_\beta(r,\theta) | \psi_\alpha(E; R_\infty, r, \theta) \rangle \tag{2}$$

Here, the scattering wave function can be written as

$$\psi_\alpha(E) = \frac{i}{2\pi} \hat{G}^+(E) |\chi_\alpha\rangle = \frac{i}{2\pi} \frac{1}{E - \hat{H} + i\hat{\gamma}} |\chi_\alpha\rangle \tag{3}$$

where $k_\beta^2 = 2\mu_\beta(E - \epsilon_\beta)/\hbar^2$ with ϵ_β being the internal energy of SH product (expressions for k_α and k_0 are similar), and

$$a_\alpha(E) = \sqrt{\frac{\mu_\alpha}{2\pi\hbar k_\alpha}} \int e^{ikR'} g(R') \mathrm{d}R' = \sqrt{\frac{\mu_\alpha}{2\pi\hbar k_\alpha}} \bar{g}(-k_\alpha)$$

with $\mu_{\alpha(\beta)}$ being the $\alpha(\beta)$ arrangement channel translational reduced mass. Equation 3 is the TI wave packet-Lippmann−Schwinger equation of Kouri et al.,[39] and is the central equation in our Lanczos method. One can compute $\psi_\alpha(E)$ either via a TD wave packet method (time propagation followed by partial Fourier transformation) or through a TI wave packet method such as expansion of the Green operator using Chebyshev polynomials.

Equation 3 can be rearranged as a linear system

$$(E - \hat{H} + i\hat{\gamma}) |\psi_\alpha(E)\rangle = \frac{i}{2\pi} |\chi_\alpha\rangle \tag{4}$$

For a large molecular system, it is nontrivial to solve this linear system. Our approach involves transforming this linear system from the primary representation to a tridiagonal (Lanczos) representation. Inside the subspace, the linear system takes the form

$$(E - \mathbf{T}_M) || \phi(E) \rangle = |e_1\rangle \tag{5}$$

which is easily solved by a *QR* algorithm. In eq 5, $\mathbf{T}_M$ is the Lanczos representation of the primary complex Hamiltonian, $\hat{H}' = \hat{H} - i\hat{\gamma}$, $|e_1\rangle$ is the first column of the $M \times M$ identity matrix, and $|\phi(E)\rangle$ is the subspace scattering wave function.

We employ the Lanczos algorithm[65] for complex-symmetric matrixes[66] to set up the Lanczos subspace. Starting with a normalized initial vector $|v_1\rangle = |\chi_\alpha\rangle$ and setting β_1=0, we use the three-term vector recursion

$$\beta_{k+1} |v_{k+1}\rangle = \hat{H}' |v_k\rangle - \alpha_k |v_k\rangle - \beta_k |v_{k-1}\rangle \tag{6}$$

to generate $\mathbf{T}_M$ with diagonal elements, $\alpha_k = (v_k|\hat{H}'|v_k)$, and subdiagonal elements, $\beta_k = (v_{k-1}|\hat{H}'|v_k)$. Note that the elements are computed with a complex-symmetric inner product (i.e., the bra states are not complex conjugated).

The initial wave packet, $|\chi_\alpha\rangle$, is chosen to be the product of a localized translational wave packet in the scattering coordinate, R' say, and a specific rovibrational eigenfunction in the remaining reactant coordinates (r' and θ' for our purposes)

$$|\chi_\alpha\rangle = g(R') \phi_v \phi_{v0}(r') P_{j0}(\theta') \tag{7}$$

with $g(R') = ((1/\pi\sigma^2))^{1/4} \exp[(-(R' - R'_0)^2/2\sigma^2)] \exp(-ik_0 R')$. The momentum representation of the translational component is analytical, and given by

$$\bar{g}(-k) = \int_0^\infty \exp(ikR') g(R') dR' = (4\pi\sigma^2)^{1/4} \left\{ \exp[i(k - k_0)R'_0] \exp\left[-\frac{\sigma^2}{2}(k - k_0)^2 \right] \right\} \tag{8}$$

Note that at this point one must transform between product Jacobi coordinates (R, r, θ) and reactant coordinates (R', r', θ') to calculate $|\chi_\alpha\rangle$ properly.

After establishing the Lanczos subspace, we calculate the quasi-minimal residual solution of the linear system in eq 5 by performing the *QR* factorization[67]

$$(E - \bar{\mathbf{T}}_M) = \mathbf{Q}_{M+1}^+ \begin{bmatrix} \mathbf{R}_M \\ 0 \end{bmatrix} \tag{9}$$

where $\mathbf{Q}_{M+1}$ is a unitary matrix ($^+$ indicates the Hermitian adjoint). Only the elements of the upper-triangular matrix $\mathbf{R}_M$ with bandwidth 3 and the vector $|\tilde{t}_{M+1}\rangle = \mathbf{Q}_{M+1}|e_1\rangle$ need to be stored. The subspace scattering wave function is obtained via

$$|\phi(E)\rangle = \mathbf{R}_M^{-1} |\tilde{t}_M\rangle \tag{10}$$

The Lanczos subspace is independent of a constant energy shift, *E*. Hence, from a *single* Lanczos subspace we are able to solve the linear system in eq 5 and obtain the representations of the scattering wave functions for any desired energy within the spectral range of the initial wave packet.

Having obtained $|\phi(E)\rangle$, it is straightforward to compute state-to-state **S** matrix elements from eq 2 since wave functions in the primary and Lanczos representations are related through

$$|\psi(E)\rangle = \mathbf{V}_M |\phi(E)\rangle = \sum_{i=1}^{M} \phi_i(E) v_i \tag{11}$$

where the orthonormal Lanczos matrix, $\mathbf{V}_M$, tridiagonalizes the primary Hamiltonian. The state-to-state reaction probabilities are now given by

$$P_{\alpha\beta}(E) = |S_{\alpha\beta}(E)|^2 = \frac{4\pi^2\hbar^2 k_\alpha k_\beta}{|\bar{g}(-k_\alpha)|^2 \mu_\alpha \mu_\beta} |D_{\alpha\beta}(E)|^2 \tag{12}$$

where the overlap integral is

$$D_{\alpha\beta}(E) = \langle\varphi_\beta(r,\theta)|\psi_\alpha(E; R_\infty, r, \theta)\rangle = \sum_{i=1}^{M}\phi_i(E)\langle\varphi_\beta(r,\theta)|\upsilon_i (R_\infty,r,\theta)\rangle = \sum_{i=1}^{M}\phi_i(E)c_i^\beta \quad (13)$$

The vectors $\{|c^\beta\rangle\}$ are the subspace versions of the primary internal SH states $|\varphi_\beta\rangle = \phi_\nu(r)P_j(\theta)$, which can be easily accumulated as the Lanczos recursion proceeds. Thus, by a single Lanczos run one can calculate *all* the state-to-state reaction probabilities from the target incoming reactant state for energies within the spectral range of the initial wave packet.

3. Results

3.1 Hamiltonian. The triatomic H_2S Hamiltonian with total angular momentum $J = 0$ is written in terms of product Jacobi coordinates

$$\hat{H} = -\frac{\hbar^2}{2\mu_{\mathrm{H,HS}}}\frac{1}{R}\frac{\partial^2}{\partial R^2}R - \frac{\hbar^2}{2\mu_{HS}}\frac{1}{r}\frac{\partial^2}{\partial r^2}r + \frac{\hbar^2}{2}\left(\frac{1}{\mu_{\mathrm{H,HS}}R^2} + \frac{1}{\mu_{\mathrm{HS}}r^2}\right)\hat{j}^2 + V(R,r,\theta) \quad (14)$$

where R is the separation of H from the center of mass of HS, r is the H−S separation, θ is the bend angle, and $\mu_{\mathrm{H,HS}}$ and μ_{HS} are reduced masses. For $V(R,r,\theta)$ we utilize the newly developed ground-state H_2S PES by Zyubin et al.[35] The PES has an equilibrium geometry of $R_e = 2.53$ a_0, $r_e = 2.54$ a_0, and $\theta_e = 1.43$ rad, and has a dissociation energy of 3.9 eV to the H + SH limit and a dissociation energy of 4.19 eV to the H_2 + S.

The Hamiltonian was then represented in a potential-optimized discrete variable representation[68] (PODVR). For the R coordinate, we used $N_R = 158$ PODVR points, which were contracted from 450 evenly spaced primitive Sinc DVR points[69] spanning the range from 0.5 a_0 to 15.5 a_0 with the one-dimensional reference potential $V(R,r_e,\theta_e)$. Similarly, for the r coordinate, $N_r = 142$ PODVR points were obtained from 426 primary DVR points spanning the range from 1.3 a_0 to 15.50 a_0 using the reference potential $V(R_e,r,\theta_e)$. For θ variable, we used $N_\theta = 43$ G-Legendre quadrature DVR points. The resulting direct product basis set was further contracted by discarding those points whose potential energies were higher than the cutoff energy $V_{\mathrm{cutoff}} = 2.4$ eV (relative to the S (^{1}D) + H_2 limit), resulting in the final basis size of 342 103.

The Hamiltonian has been augmented in the R and r coordinates with a complex absorbing potential to incorporate the necessary dissipative boundary conditions. The absorbing potential takes the following form ($z = R, r$)

$$\hat{\gamma}(z) = \frac{\gamma_0}{\cosh^2[((z_{\max} - z))/\lambda]} \quad (15)$$

Where $z_{\max}$ is the maxima in R or r coordinate, and γ_0 and λ are two adjusting parameters. In this calculation $z_{\max} = 15.5$ a_0, $\gamma_0 = 2.0$ eV, and $\lambda = 0.5$ a_0 in both R and r coordinate.

3.2 Analysis for $J = 0$ Case. Using the method described in section 2, first we set up a Lanczos subspace of $M = 40\,000$. Then we perform final state to state analysis within the subspace at thousands of scattering energies from 0.26 to 0.60 eV. The convergence of the method has been checked in respect to both the size of the Lanczos subspace and the basis size. $M = 40\,000$ Lanczos iterations provide good converge of most of the state-to-state reaction probabilities at this energy range, and even at $M = 20\,000$, the basic profile of the reaction probabilities has appeared. Further iterations can only resolve some narrow individual resonances better. During the calculations, we can monitor the error norms for the subspace representations of the scattering waves (i.e., at energy E the error norm ρ is given by $\rho = ||(\mathbf{T}_M - E)|\phi(E)\rangle - |e_1\rangle||$) as a further check of convergence. For $M = 40\,000$ the error norms for most scattering energies have dropped to below 10^{-5}. We have also run the calculations with a larger angular basis size $N_\theta = 86$. The calculations are much more time-consuming and the resulting energy profiles of the reaction probabilities are similar to those for the $N_\theta = 43$ calculations, indicating that the smaller angular basis is adequate. Thus, we believe $M = 40\,000$ and $N_\theta = 43$ are quite sufficient for converging most of the state-to-state reactive probabilities and total reaction probabilities and the results presented below are for these values of the parameters. All state-to-state reactive probabilities associated with the ground H_2 reactant state ($\nu_0 = 0$, $j_0 = 0$) and ground SH product states ($\nu = 0$, j) with $j = 0-23$ as well as vibrationally excited product SH states ($\nu = 1$, j) with $j = 0-16$ have been calculated and are selectively presented in Figure 1. It is apparent that the reaction probabilities are dominated by resonances, most of them are overlapping ones. This is a clear manifestation of the complex forming and decaying process. Analysis of some resonance widths indicates the lifetime of the resonances is in the order of picosecond.

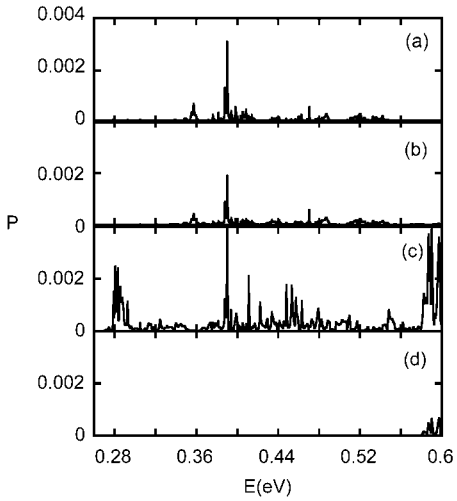

Figure 1. (a) Calculated state-to-state reactive probabilities from the ground state of H_2 ($\nu_0 = 0$, $j_0 = 0$) to product SH states ($\nu = 0$, j) with $j = 0$. Here, the energy E is defined as the internal energy of the diatom plus the translational energy. (b) Same as (a), but for product SH states ($\nu = 1$, j) with $j = 0$. (c) Same as (a), but for product SH states ($\nu = 0$, j) with $j = 15$. (d) Same as (a), but for product SH states ($\nu = 1$, j) with $j = 15$.

Figure 2 shows two selected rotational state distributions of the product SH ($\nu = 0$) at scattering energy $E = 0.3656$ eV (a), and at $E = 0.4403$ eV (b). The general feature is that the distributions show a very complicated oscillatory behavior, with the number of oscillations generally increasing with energy. The fluctuations in the distributions seem to be random and unpredictable from energy to energy. (We have calculated the rotational state distributions for all $\nu = 0$ and $\nu = 1$ open channels for 2000 scattering energies lying between 0.26 eV to 0.6 eV. For brevity, only two of them have been reported.) This fluctuation behavior indicates that statistical theory may be

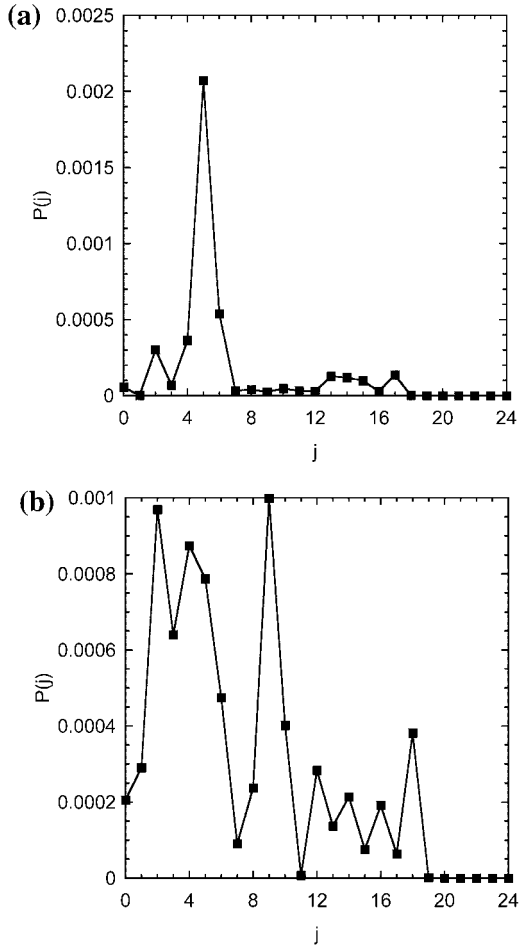

Figure 2. (a) Rotational state distributions of the product SH ($v = 0$) for $E = 0.3656$ eV. (b) Similar to (a), but for $E = 0.4403$ eV.

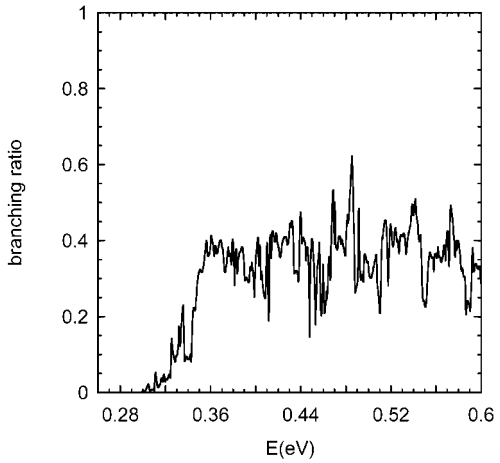

Figure 3. Vibrational branching ratio between SH $v = 1$ and $v = 0$ vibrational levels.

employed to interpret the more averaged quantities such as rate constant, but not the detailed product state distributions. Although the features are sensitive to the specific scattering energy, it is evident that the reaction tends to favor the production of rotationally excited SH.

In Figure 3 we plot the branching ratio of rotation-summed reaction probabilities for the product SH $v = 1$ and $v = 0$ vibrational levels. At this energy range only two vibrational channels have opened. From this figure, we can see that this reaction only produces a small fraction of vibrationally excited SH product. The vibrational distributions fluctuate between

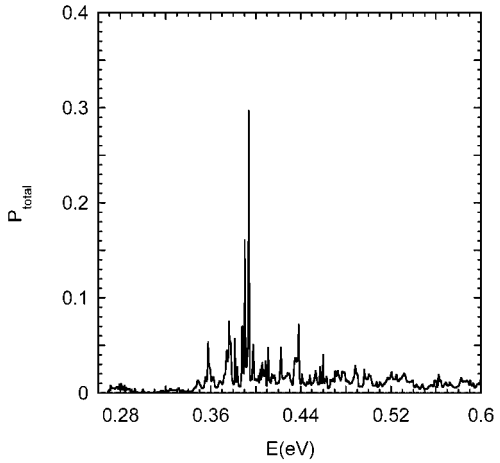

Figure 4. Total reaction probabilities as a function of energy for the ground rovibrational H_2 state.

energies, but the general trend is that the ratio increases with energy at low energies, then oscillates severely around an average value.

After acquiring all the state-to-state reaction probabilities from H_2 ($v_0 = 0, j_0 = 0$) to all the energetically accessible SH product states, it is straightforward to calculate total reaction probabilities from a given reactant state. In Figure 4, we plot the total reaction probabilities from the ground rovibrational H_2 state in the energy range from 0.26 to 0.6 eV. As can be expected, the total reaction probabilities are dominated by overlapping resonances, similar to state to state reaction probabilities.

3.3 Estimation of Reaction Cross Sections. The calculation of an integral reactive cross section requires knowledge of reaction probabilities for a large range of total angular momenta. Because it is very expensive to calculate such reaction probabilities for different $J > 0$ cases, we will employ a J-shifting method[58,59] for higher J values $P(E,J) = \sum_{K=-J}^{J} P(E - \epsilon_{\text{rot}}^{JK}, 0)$. Here $\epsilon_{\text{rot}}^{JK} = [J(J+1) - 2K^2](\hbar^2/2\mu R''^2)$. To determine the transitional state geometry more reasonably for a potential without a barrier, we calculate the JK dependent centrifugal barriers in the entrance channel $V_{JK}(R) = \langle v_0, j_0 | V | v_0, j_0 \rangle + [J(J+1) - 2K^2](\hbar^2/2\mu R''^2)$, which was taken as the geometry of the transitional state. In our calculations, we take the approximation $R'' = 2.14a_0$. After computing different $P(E,J)$, we can calculate the integral reaction cross section as

$$\sigma(E_{tr}; v_0, j_0) = \frac{1}{g}\frac{\pi}{k_{tr}^2}\sum_{J=0}^{\infty}(2J+1)P(E_{tr},J; v_0, j_0) \qquad (16)$$

where $k_{tr} = \sqrt{2\mu E_{tr}}/\{\hbar\}$, and the electronic degeneracy g is 5 for H_2S. In this calculation, we only consider the reaction probabilities from the ground-state H_2 ($v_0 = 0$, $j_0 = 0$). This approximation is generally consistent with the molecular beam experiment conditions,[32] in which the average rotational energy of the target molecules is about 0.3 kcal/mol. The calculated excitation functions below 4.1 kcal/mol are presented in Figure 5, where the experimental data is also available. The general agreement among the quantum mechanical results, the QCT calculations[34] and the experimental data is clearly apparent. The excitation functions decrease with increasing collision energy, which is typical of an insertion mechanism. However, embedded on the curve of the excitation functions are thousands of small resonance structures, which did not show up in experimental data and QCT results. This is most likely because we use the J-shifting to estimate the $J > 0$ reaction probabilities, thus all

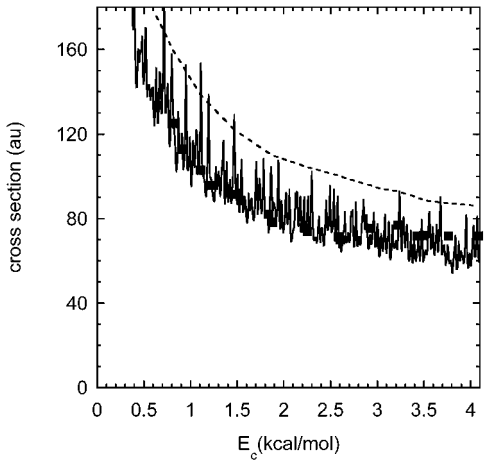

Figure 5. Comparison of excitation functions calculated in this work with the experimental results and QCT excitation functions. Solid line represents quantum results; dashed line is from QCT calculations; and the solid squares are the experimental data.

resonances in $J = 0$ reaction probabilities appear in $J > 0$ reaction probabilities. Evidence from rigorous calculations at nonzero values of total J in the H + O_2 reaction[70,71] indicates that the sharp resonance structure of the $J = 0$ reaction probability profiles tends to wash out at $J > 0$.

4. Conclusion

In this paper, we have applied a Lanczos subspace time-independent wave packet method to the S(^{1}D) + H_2 reactive scattering process. In our method, the TI wave packet-Lippmann−Schwinger equation is first transformed from the primary representation into a Lanczos subspace, within which we solve the tridiagonal linear system for the action of the Green operator by a QR algorithm. From a single Lanczos run, all the state-to-state **S** matrix elements, product state distributions and total reaction probabilities from a given reactant channel wave packet can be obtained at any desired energy in the spectral range of the initial wave packet.

The results indicate that S (^{1}D) + H_2 scattering is dominated by resonances (most of them are overlapping). Analysis of some resonance widths indicates the complex lifetime of the resonances is in the order of picosecond. The interferences among the resonances lead to very complicated reaction dynamics, which is manifested in the fluctuations of both product rotational state distributions and vibrational branching ratios. The reaction mainly produces rotationally excited SH products with only a small fraction in vibrationally excited states.

Integral reaction cross sections of this reaction are estimated by *J*-shifting method. Comparison with QCT calculations and experimental data indicates general agreement. However, the fine resonance structures exhibited in the quantum results, which are not seen experimentally, illustrate the limitations of *J*-shifting method. Further rigorous quantum calculations for $J > 0$ are presently under investigation in our lab.

Acknowledgment. We wish to thank Professor Kopin Liu for helpful discussions concerning the experimental studies of the title reaction. We thank Professor Rex T. Skodje and Dr. Sheng Der Chao for sending the H_2S PES code, and Professor Herschel Rabitz and Dr. Tak-San Ho for provision of the RKHS fitting code. We are grateful to the University of Queensland, the Institute of Atomic and Molecular Sciences (Academia Sinica, Taipei, Taiwan) and the Australian Research Council for supporting this work.

References and Notes

(1) Buss, R. J.; Casavecchia, P.; Hirooka, T.; Sibener, S. J.; Lee, Y. T. *Chem. Phys. Lett.* **1981**, *82*, 386.
(2) Laurent, T.; Naik, P. D.; Volpp, H. R.; Wolfrum, J.; Arusi-Parpar, T.; Bar, I.; Rosenwaks, S. *Chem. Phys. Lett.* **1995**, *236*, 343.
(3) Alexander, A. J.; Aoiz, F. J.; Brouard, M.; Burak, I.; Fujimura, Y.; Short, J.; Simons, J. P. **1996**, *262*, 589.
(4) Hsu, Y.-T.; Liu, K. *J. Chem. Phys.* **1997**, *107*, 1664.
(5) Hsu, Y.-T.; Wang, J.-H.; Liu, K. *J. Chem. Phys.* **1997**, *107*, 2351.
(6) Alexander, A. J.; Blunt, D. A.; Brouard, M.; Simons, J. P.; Aoiz, F. J.; Banares, L.; Fujimura, Y.; Tsubouchi, M. *Faraday Discuss.* **1997**, *108*, 375.
(7) Alagia, M.; Balucani, N.; Cartechini, L.; Casavecchia, P.; Kleef, E. H. v.; Volpi, G. C.; Kuntz, P. J.; Sloan, J. J. *J. Chem. Phys.* **1998**, *108*, 6698.
(8) Ahmed, M.; Peterka, D. S.; Suits, A. G. *Chem. Phys. Lett.* **1999**, *301*, 372.
(9) Lee, S.-H.; Liu, K. *J. Chem. Phys.* **1999**, *111*, 4351.
(10) Hsu, Y.-T.; Liu, K.; Pederson, L. A.; Schatz, G. C. *J. Chem. Phys.* **1999**, *111*, 7921.
(11) Hermine, P.; Hsu, Y.-T.; Liu, K. *Phys. Chem. Chem. Phys.* **2000**, *2*, 581.
(12) Liu, X.; Lin, J. J.; Harich, S. A.; Yang, X. *J. Chem. Phys.* **2000**, *113*, 1325.
(13) Fitzcharles, M. S.; Schatz, G. C. *J. Phys. Chem.* **1986**, *90*, 3634.
(14) Walch, S. P.; Harding, L. B. *J. Chem. Phys.* **1988**, *88*, 7653.
(15) Goldfield, E. M.; Wiesenfeld, J. R. *J. Chem. Phys.* **1990**, *93*, 1030.
(16) Schatz, G. C.; Papaioannou, A.; Peterson, L. A.; Harding, L. B.; Ho, T.-S.; Hollebeek, T.; Rabitz, H. **1997**, *107*, 2340.
(17) Alexander, A. J.; Aoiz, F. J.; Banares, L.; Brouard, M.; Simons, J. P. *Phys. Chem. Chem. Phys.* **2000**, *2*, 571.
(18) Whitlock, P. A.; Muckerman, J. T.; Fisher, E. R. *J. Chem. Phys.* **1982**, *76*, 4468.
(19) Kuntz, P. J.; Niefer, B. I.; Sloan, J. J. *J. Chem. Phys.* **1988**, *88*, 3629.
(20) Kuntz, P. J.; Niefer, B. I.; Sloan, J. J. *Chem. Phys.* **1991**, *151*, 77.
(21) Schatz, G. C.; Pederson, L. A.; Kuntz, P. J. *Faraday Discuss.* **1997**, *108*, 357.
(22) Badenhoop, J. K.; Koizumi, H.; Schatz, G. C. *J. Chem. Phys.* **1989**, *91*, 142.
(23) Peng, T.; Zhang, D. H.; Zhang, J. Z. H.; Schinke, R. *Chem. Phys. Lett.* **1996**, *248*, 37.
(24) Dai, J. *J. Chem. Phys.* **1997**, *107*, 4934.
(25) Balint-Kurti, G. G.; Gonzalez, A. I.; Goldfield, E. M.; Gray, S. K. *Faraday Discuss.* **1998**, *110*, 169.
(26) Gray, S. K.; Goldfield, E. M.; Schatz, G. C.; Balint-Kurtii, G. G. *Phys. Chem. Chem. Phys.* **1999**, *1*, 1141.
(27) Drukker, K.; Schatz, G. C. *J. Chem. Phys.* **1999**, *111*, 2451.
(28) Schinke, R.; W. A. Lester, J. *J. Chem. Phys.* **1980**, *72*, 3754.
(29) Murrell, J. N.; Carter, S. *J. Phys. Chem.* **1984**, *88*, 4887.
(30) Ho, T.-S.; Hollebeek, T.; Rabitz, H.; Harding, L. B.; Schatz, G. C. *J. Chem. Phys.* **1996**, *105*, 10 472.
(31) Dobbyn, A. J.; Knowles, P. J. *Mol. Phys.* **1997**, *91*, 1107.
(32) Lee, S. H.; Liu, K. *Chem. Phys. Lett.* **1998**, *290*, 323.
(33) Lee, S. H.; Liu, K. *J. Phys. Chem. A* **1998**, *102*, 8637.
(34) Chao, S. D.; Skodje, R. T. *J. Phys. Chem. A* **2001**, *105*, 2474.
(35) Zyubin, A. S.; Mebel, A. M.; Chao, S. D.; Skodje, R. T. *J. Chem. Phys.* **2001**, *114*, 320.
(36) Chang, A. H. H.; Lin, S. H. *Chem. Phys. Lett.* **2000**, *320*, 161.
(37) Hollebeek, T.; Ho, T. S.; Rabitz, H. *Annu. Rev. Phys. Chem.* **1999**, *50*, 537.
(38) Light, J. C.; Hamilton, I. P.; Lill, J. V. *J. Chem. Phys.* **1985**, *82*, 1400.
(39) Kouri, D. J.; Arnold, M.; Hoffman, D. K. *Chem. Phys. Lett.* **1993**, *203*, 166.
(40) Huang, Y.; Zhu, W.; Kouri, D. J.; Hoffman, D. K. *Chem. Phys. Lett.* **1993**, *206*, 96.
(41) Zhu, W.; Huang, Y.; Kouri, D. J.; Arnold, M.; Hoffman, D. K. *Phys. Rev. Lett.* **1994**, *72*, 1310.
(42) Mandelshtam, V. A.; Taylor, H. S. *J. Chem. Phys.* **1995**, *103*, 2903.
(43) Mandelshtam, V. A.; Grozdanov, T. P.; Taylor, H. S. *J. Chem. Phys.* **1995**, *103*, 10 074.
(44) Mandelshtam, V. A.; Taylor, H. S. *J. Chem. Phys.* **1995**, *102*, 7390.
(45) Chen, R.; Guo, H. *J. Chem. Phys.* **1996**, *105*, 3569.
(46) Chen, R.; Guo, H. *J. Chem. Phys.* **1999**, *111*, 464.
(47) Kroes, G.-J.; Neuhauser, D. *J. Chem. Phys.* **1996**, *105*, 9104.
(48) Kroes, G.-J.; Neuhauser, D. *J. Chem. Phys.* **1996**, *105*, 8690−8698.
(49) McCormack, D. A.; Kroes, G.-J.; Neuhauser, D. *J. Chem. Phys.* **1998**, *109*, 5177.
(50) Gray, S. K.; Balint-Kurti, G. G. *J. Chem. Phys.* **1998**, *108*, 950.
(51) Hankel, M.; Balint-Kurti, G. G.; Gray, S. K. *J. Chem. Phys.* **2000**, *113*, 9658.

(52) Zhang, H.; Smith, S. C. *J. Chem. Phys.* **2002**, *116*, 2354.
(53) Yu, H. G.; Smith, S. C. *Ber. Bunsen-Ges. Phys. Chem.* **1997**, *101*, 400.
(54) Yu, H. G.; Smith, S. C. *J. Chem. Phys.* **1997**, *107*, 9985.
(55) Yu, H. G.; Smith, S. C. *Chem. Phys. Lett.* **1998**, *283*, 69.
(56) Yu, H.-G.; Smith, S. C. *J. Comput. Phys.* **1998**, *143*, 484−494.
(57) Zhang, H.; Smith, S. C. *Phys. Chem. Chem. Phys.* **2001**, *3*, 2282.
(58) Bowman, J. M. *J. Phys. Chem.* **1991**, *95*, 4960.
(59) Sun, Q.; Bowman, J. M.; Schatz, G. C.; Sharpe, J. R.; Connor, J. N. L. *J. Chem. Phys.* **1990**, *92*, 1677.
(60) Weeks, D. E.; Tannor, D. J. *Chem. Phys. Lett.* **1993**, *207*, 301.
(61) Tannor, D. J.; Garashchuk, S. *Annu. Rev. Phys. Chem.* **2000**, *51*, 553.
(62) Tannor, D. J.; Weeks, D. E. *J. Chem. Phys.* **1993**, *98*, 3884−3893.
(63) Kouri, D. J.; Huang, Y.; Zhu, W.; Hoffman, D. K. *J. Chem. Phys.* **1994**, *100*, 3662−3671.
(64) Zhang, J. Z. H. *Theory and Application of Quantum Molecular Dynamics*; World Scientific, 1999.
(65) Lanczos, C. *J. Res. Natl. Bur. Stand.* **1950**, *45*, 255.
(66) Moro, G.; Freed, J. H. *J. Chem. Phys.* **1981**, *74*, 3757.
(67) Freund, R. W. *SIAM J. Sci. Stat. Comput.* **1992**, *13*, 425.
(68) Echave, J.; Clary, D. *Chem. Phys. Lett.* **1992**, *190*, 225.
(69) Colbert, D. T.; Miller, W. H. *J. Chem. Phys.* **1992**, *96*, 1982.
(70) Meijer, A.; Goldfield, E. M. *J. Chem. Phys.* **1998**, *108*, 5404.
(71) Meijer, A.; Goldfield, E. M. *J. Chem. Phys.* **1999**, *110*, 870.